

1 **Comparison of the multifractal characteristics of heavy**
2 **metals in soils within two areas of contrasting economic**
3 **activities in China**

4 Xiaohui Li^{a, b}, Xiangling Li^a, Feng Yuan^{a, b*}, Simon M. Jowitt^{c, d}, Taofa Zhou^a, Kui
5 Yang^a, Jie Zhou^a, Xunyu Hu^a, Yang Li^a

6 a. School of Resources and Environmental Engineering, Hefei University of
7 Technology, Hefei 230009, China

8 b. Xinjiang Research Centre for Mineral Resources, Xinjiang Institute of Ecology and
9 Geography, Chinese Academy of Sciences, Urumqi, Xinjiang 830011, China

10 c. School of Earth, Atmosphere and Environment, Monash University, Wellington
11 Road, Clayton, VIC 3800, Australia

12 d. Department of Geoscience, University of Nevada Las Vegas, 4505 S. Maryland
13 Parkway, Las Vegas, NV 89154-4010, USA

14 *Corresponding author: Email: yf_hfut@163.com, Tel: +8605512901648

15 **Abstract**

16 Industrial and agricultural activities can generate heavy metal pollution that can
17 cause a number of negative environmental and health impacts. This means that
18 evaluating heavy metal pollution and identifying the sources of these pollutants,
19 especially in urban or developed areas, is an important first step in mitigating the
20 effects of these contaminating but necessary economic activities. Here, we present the
21 results of a heavy metal (Cu, Pb, Zn, Cd, As and Hg) soil geochemical survey in Hefei
22 city and use a multifractal spectral technique to identify and compare the
23 multifractality of heavy metal concentrations of soils within the industrial Daxing and
24 agricultural Yicheng areas. This paper uses three multifractal parameters ($\Delta\alpha$, $\Delta f(\alpha)$
25 and $\tau''(1)$) for these soil geochemical data to indicate the overall amount of

26 multifractality within the soil geochemical data. The results show all of the elements
27 barring Hg have larger $\Delta\alpha$, $\Delta f(\alpha)$ and $\tau''(1)$ values in the Daxing area compared to the
28 Yicheng area. The differences in the degree of multifractality between Daxing and
29 Yicheng areas indicate that the soils in these areas have differing multifractal
30 geochemical characteristics, suggesting that the differing economic activities in these
31 areas generate very different heavy metal pollutant loads. In addition, the industrial
32 Daxing area contains significant Pb and Cd soil contamination, whereas Hg is the
33 main heavy metal present in soils within the Yicheng area, indicating that differing
34 clean-up procedures and approaches to remediating these polluted areas are needed.
35 The results also indicate that multifractal modeling and the associated generation of
36 multifractal parameters can be a useful approach in the evaluation of heavy metal
37 pollution in soils.

38

39 **Keywords:** soil geochemistry; multifractal modelling; heavy metal pollution; Hefei

40

41 **1. Introduction and overview of the study area**

42 Heavy metal pollution within soil poses a serious risk for human health and the
43 environment, and thus soil pollution caused by anthropogenic activities (including
44 industry and agriculture) has been the focus of a significant amount of research (e.g.,
45 [Leyval et al., 1997](#); [Thomas and Stefan, 2002](#); [McGrath et al., 2004](#); [Wang et al., 2007](#);
46 [Luo et al., 2011](#)). Analyzing soil geochemistry and pollution using multifractal
47 techniques can investigate many of the problems of nonlinear variability which
48 commonly arise when dealing with pollutants and as well as enabling the
49 identification of non-linear characteristics within datasets. This approach can yield
50 new information that can be used to understand the factors controlling the distribution
51 of key elements within the objects or data being studied ([Salvadori, 1997](#); [Gonçalves,](#)
52 [2000](#); [Zuo et al., 2012](#)). This in turn means that determining the multifractal
53 characteristics of the distribution of heavy metals in soils can improve our
54 understanding of any heavy metal pollution that is associated with these differing

55 anthropogenic activities.

56 Multifractal techniques include singularity mapping and multifractal
57 interpolation that enable more detailed analysis of the spatial distribution of heavy
58 metals, concentration-area modeling that can be used to define threshold values
59 between background (i.e. geological) and anthropogenic anomalies (Lima et al., 2003),
60 spectral density-area modeling that can be used to define thresholds to separate
61 anomalies (i.e., anthropogenically derived heavy metal concentrations in this case)
62 from background concentrations (i.e., geologically derived heavy metal
63 concentrations; Cheng, 2001), and multifractal spectra that highlights non-linear
64 characteristics and identifies anomalous behavior that reflects the characteristics of
65 some multifractal sets (Gonçalves, 2000; Albanese et al., 2007; Guillén et al., 2011),
66 such as the presence of porous structures and spatial variations in soil properties
67 (Caniego et al., 2005; Dathe et al., 2006). This means that multifractal techniques can
68 be useful tools for the analysis of heavy metal pollution within soils (e.g., Salvadori et
69 al., 1997; Lima et al., 2003; Albanese et al., 2007; Guillén et al., 2011). These
70 multifractal techniques are not only used in environmental science, but also in a
71 number of differing fields, including geophysics (Schertzer et al., 2011), medicine
72 (Jennane et al., 2001), computer science (Wendt et al., 2009), geology (Cheng, 1995;
73 Deng et al., 2011; Zuo et al., 2012, 2014; Yuan et al., 2012, 2015; Nazarpour et al.,
74 2014) and ecology (Scheuring and Riedi, 1994; Pascual et al., 1995), among others.

75 Hefei is the capital of Anhui Province, China, and has an urban area that includes
76 the towns of Daxing and Yicheng, which focus on industrial and agricultural activities,
77 respectively. Here, we use multifractal spectra techniques and three parameters ($\Delta\alpha$,
78 $\Delta f(\alpha)$ and $\tau''(1)$) to analyze and compare the degree and characteristics of the
79 multifractality of heavy metal contamination in soils associated with anthropogenic
80 activities in this region. The results will further enable and inform future planning for
81 any necessary remediation of the soils in the Daxing and Yicheng areas.

82 **2. Study area and geochemical data**

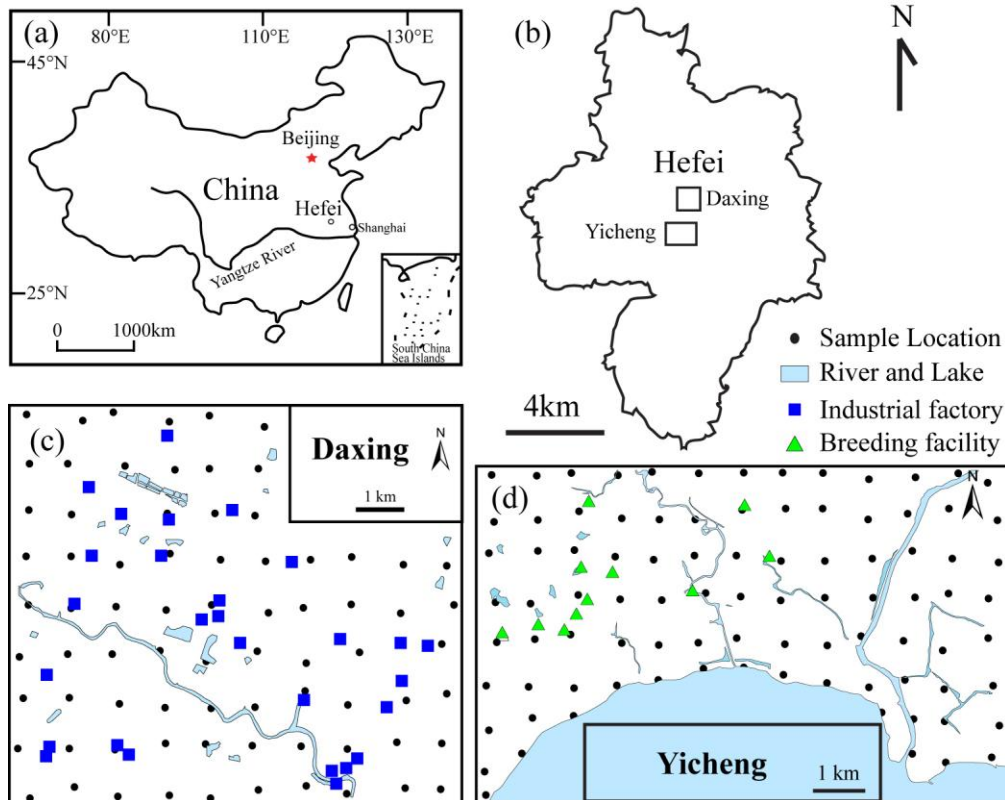
83 **2.1 Study area**

84 The city of Hefei is situated in central–eastern China (Fig. 1(a)), has
85 approximately 7.7 million inhabitants and covers an area of around 11,408 km². This
86 paper focuses on the towns of Daxing and Yicheng (Fig. 1(b)), with the former
87 representing one of the traditional industrial areas of Hefei and containing numerous
88 factories that are involved in the steel industry, chemical industry, paper making, and
89 the production of furniture and construction materials, among others. In contrast, the
90 town of Yicheng focuses its economic activities on agricultural production, byproduct
91 processing, livestock and poultry breeding, ornamentals, and other enterprises related
92 to agricultural activity.

93 **2.2 Sampling and analysis**

94 The study areas are covered by Quaternary sedimentary soils and are free of both
95 natural mineralization and mining-related contamination. A total of 169 surface (<20
96 cm depth) soil samples were taken from the towns of Daxing and Yicheng on 1 × 1
97 km grids, yielding 78 samples from Daxing and 91 samples from Yicheng (Fig.
98 1(c–d)). Sampling errors were minimized by splitting each sample into 3–5
99 sub-samples, each of which weighed more than 500 g. Each of these sub-samples was
100 air-dried before being broken up using a wooden roller and then sieved to pass
101 through a 0.85 mm mesh. The concentrations of 6 heavy metal elements (Cu, Pb, Zn,
102 Cd, As and Hg) were determined during this study, with Cd, Cu, Pb and Zn
103 concentrations determined by inductively coupled plasma–mass spectrometry
104 (ICP–MS), whereas Hg and As concentrations were determined by hydride
105 generation–atomic fluorescence spectrometry (AFS; Armstrong et al., 1999;
106 Gómez-Ariza et al., 2000). These techniques have detection limits of 1 ppm for Cu, 2
107 ppm for Pb and Zn, 30 ppb for Cd, 0.5 ppm for As and 5 ppb for Hg. The accuracy of
108 these data was monitored by repeat and replicate determinations using instrumental
109 neutron activation analysis (INAA), with analytical precision was monitored using
110 variance of the results obtained from duplicate analyses.

111



112
113
114
115
116

Fig. 1. Location of Hefei in central-eastern China (a); location of the study areas within Hefei (b); the 1 × 1 km grids used for soil sampling in the towns of Daxing (c) and Yicheng (d)

117 3. Multifractal spectrum analysis

118 Multifractal formalisms can decompose self-similar measures into intertwined
119 fractal sets that are characterized by singularity strength and fractal dimensions
120 (Cheng, 1999). Using multifractal techniques allows non-linear characteristics within
121 datasets to be identified, enabling the extraction of information that can be used to
122 understand the factors controlling the distribution of key elements within the data.
123 Fractal spectra ($f(\alpha)$) are formalisms that can be used to describe the multifractal
124 characteristics of a dataset and can be estimated using box-counting based moment,
125 gliding box, histogram and wavelet methods, among others (Cheng, 1999; Lopes and
126 Betrouni, 2009). The most widely used of these methods are the box-counting and
127 gliding box methods, both of which are based on the moment method.

128 The calculation of the mass exponent function $\tau(q)$ for the gliding box method is
129 different from the box-counting method, with the gliding box method providing a

130 useful approach that can increase the number of samples that are available for
 131 statistical estimation within a dataset (Buczowski et al., 1998; Tarquis et al., 2006;
 132 Xie et al., 2010). This means that the gliding box approach often provides better
 133 results with lower uncertainties than the box-counting method (Cheng, 1999). As such,
 134 we have used the gliding box approach during this study. The calculation of the mass
 135 exponent function $\tau(q)$ for the gliding box method uses a partition function as follows
 136 (Cheng, 1999):

$$137 \quad \langle \tau(q) \rangle + D = \lim_{\varepsilon \rightarrow 0} \left(\frac{\log(\mu^q(\varepsilon))}{\log(\varepsilon)} \right) = \lim_{\varepsilon \rightarrow 0} \left(\frac{\log \left(\frac{1}{N^*(\varepsilon)} \sum_{i=1}^{N^*(\varepsilon)} \mu_i^q(\varepsilon) \right)}{\log(\varepsilon)} \right) \quad (1)$$

138 where $\mu_i(\varepsilon)$ denotes a measure with the i_{th} cell of a gliding box of size ε , q is the order
 139 moment of this measure, $\langle \rangle$ indicates the statistical moment, and $N^*(\varepsilon)$ indicates the
 140 total number of gliding boxes of size ε with $\mu_i(\varepsilon)$ values different from 0.

141 The values of $\tau(q)$ derived using this equation can be then used to determine α
 142 and $f(\alpha)$ values using a Legendre transformation, as expressed below:

$$143 \quad \alpha(q) = \frac{d\tau(q)}{dq} \quad (2)$$

$$144 \quad f(\alpha) = q\alpha(q) - \tau(q) = q \frac{d\tau(q)}{dq} - \tau(q) \quad (3)$$

145 $\Delta\alpha$ and Δf are essential parameters required to analyze the multifractal
 146 characteristics of the dataset in question. The widths of the left and right branches
 147 within the multifractal spectra are then defined using the following equations:

$$148 \quad \Delta\alpha_L = \alpha_0 - \alpha_{m i} \quad (4)$$

$$149 \quad \Delta\alpha_R = \alpha_{m a x} - \alpha_0 \quad (5)$$

$$150 \quad \Delta\alpha = \alpha_{m a x} - \alpha_{m i} \quad (6)$$

151 and the height difference $\Delta f(\alpha)$ between the two ends of the multifractal spectrum is
 152 then extracted using:

$$153 \quad \Delta f(\alpha) = f(\alpha_{m a x}) - f(\alpha_{m i}) \quad (7)$$

154 Higher $\Delta\alpha$ and $\Delta f(\alpha)$ values are generally indicative of datasets with more
155 heterogeneous patterns (ordered, complex, clustered) and higher levels of
156 multifractality (Cheng, 1999; Kravchenko et al., 1999). In addition, local
157 multifractality $\tau''(1)$, can also be used as a measure to quantitatively characterize the
158 multifractality of a dataset using equation 8, where ordinary spatial analysis functions
159 (autocorrelations and semivariograms) are related to low order statistical moments (0
160 to 2nd) that may determine $\tau''(1)$ (Cheng, 2006):

$$161 \quad \tau''(1) = \tau(2) - 2\tau(1) + \tau(0) \quad (8)$$

162 If μ is a multifractal and $-D < \tau''(1) < 0$, where D is the gliding-box dimension,
163 then more negative values of $\tau''(1)$ are indicative of higher degrees of multifractality,
164 whereas otherwise $\tau''(1) = 0$ for a single fractal.

165 Here, we use the three multifractal parameters described above ($\Delta\alpha$, $\Delta f(\alpha)$ and
166 $\tau''(1)$) to better identify the degrees of multifractality within the soil geochemical data
167 for the study area as well as enabling the comparison of the multifractality of differing
168 elements in the soils in this region.

169 **4. Geochemical analysis results**

170 A statistical summary of the soil geochemical data for the study area is given in
171 [Table 1](#). Samples from the Daxing area have higher Cu, Pb, Zn, Cd and As maximum,
172 mean, standard deviation, skewness, and kurtosis values than soil samples from the
173 Yicheng area, whereas the Yicheng area has a higher maximum Hg concentration
174 value than the Daxing area. In addition, the soil samples from Daxing have much
175 higher coefficient of variation (CV) values for Cu, Pb, Zn, Cd and As than the
176 samples from the Yicheng area, indicating that soils in the Daxing area contain higher
177 and more variable concentrations of these elements. This also suggests that samples
178 from the Daxing area containing elevated concentrations of heavy metals were
179 probably contaminated by anthropogenic activity.

180 All of the elements (barring Pb and Cu in the Yicheng area) in both the Yicheng
181 and Daxing areas yielded concentration histograms that are positively skewed and
182 contain some outliers (Fig. 2), indicating that these data have non-normal and

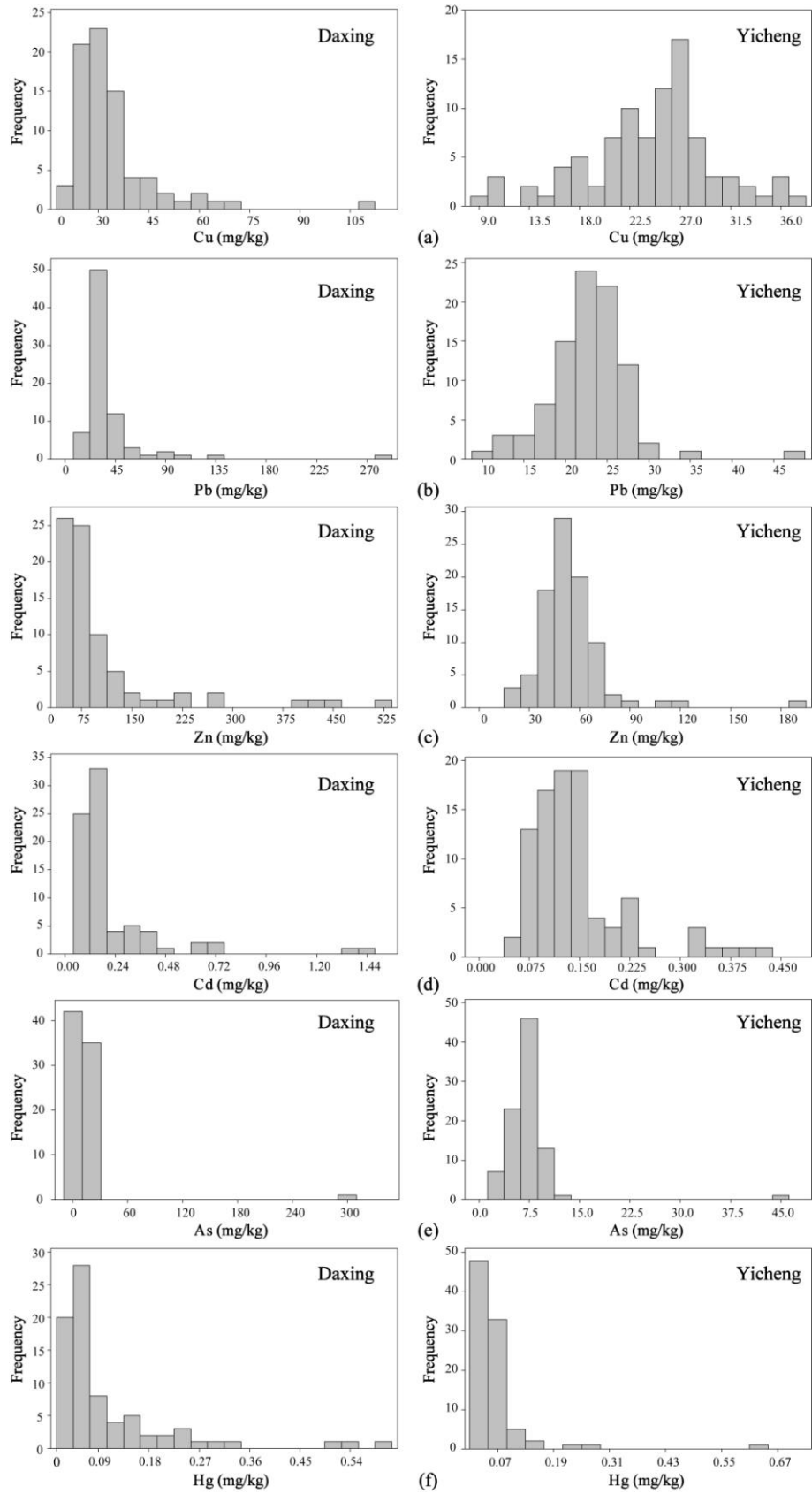
183 potentially fractal- or multifractal-type distributions. This means that multifractal
 184 techniques are highly suited for the characterization of the geochemistry of the soils
 185 and discrimination of the differing types of human activities ongoing in each area.

186

187 Table 1. Summary statistics of soil heavy metal concentrations within samples from the Daxing
 188 and Yicheng areas.

Town	Element	Min	Max	Mean	Standard deviation	Skewness	Kurtosis	CV*
		(mg/kg)	(mg/kg)	(mg/kg)	-	-	-	(%)
Daxing	Cu	19.00	111.50	33.87	13.26	3.20	14.93	39.16
	Pb	18.90	291.30	39.57	35.03	5.37	35.41	88.51
	Zn	40.90	526.10	105.8	94.40	2.91	8.59	89.19
	Cd	0.045	1.48	0.23	0.24	3.45	13.81	108.23
	As	4.93	308.20	13.97	33.89	8.72	76.64	242.56
	Hg	0.03	0.60	0.11	0.11	2.68	7.78	107.29
Yicheng	Cu	9.60	37.80	24.34	5.77	-0.38	0.41	23.71
	Pb	10.40	46.30	22.77	4.91	0.87	5.51	21.56
	Zn	20.80	194.80	54.70	21.43	3.45	20.27	39.17
	Cd	0.054	0.43	0.15	0.08	1.84	3.49	51.85
	As	2.30	44.20	7.29	4.39	6.68	56.55	60.24
	Hg	0.02	0.62	0.06	0.07	5.75	41.26	113.09

189 *CV: coefficient of variation.



190

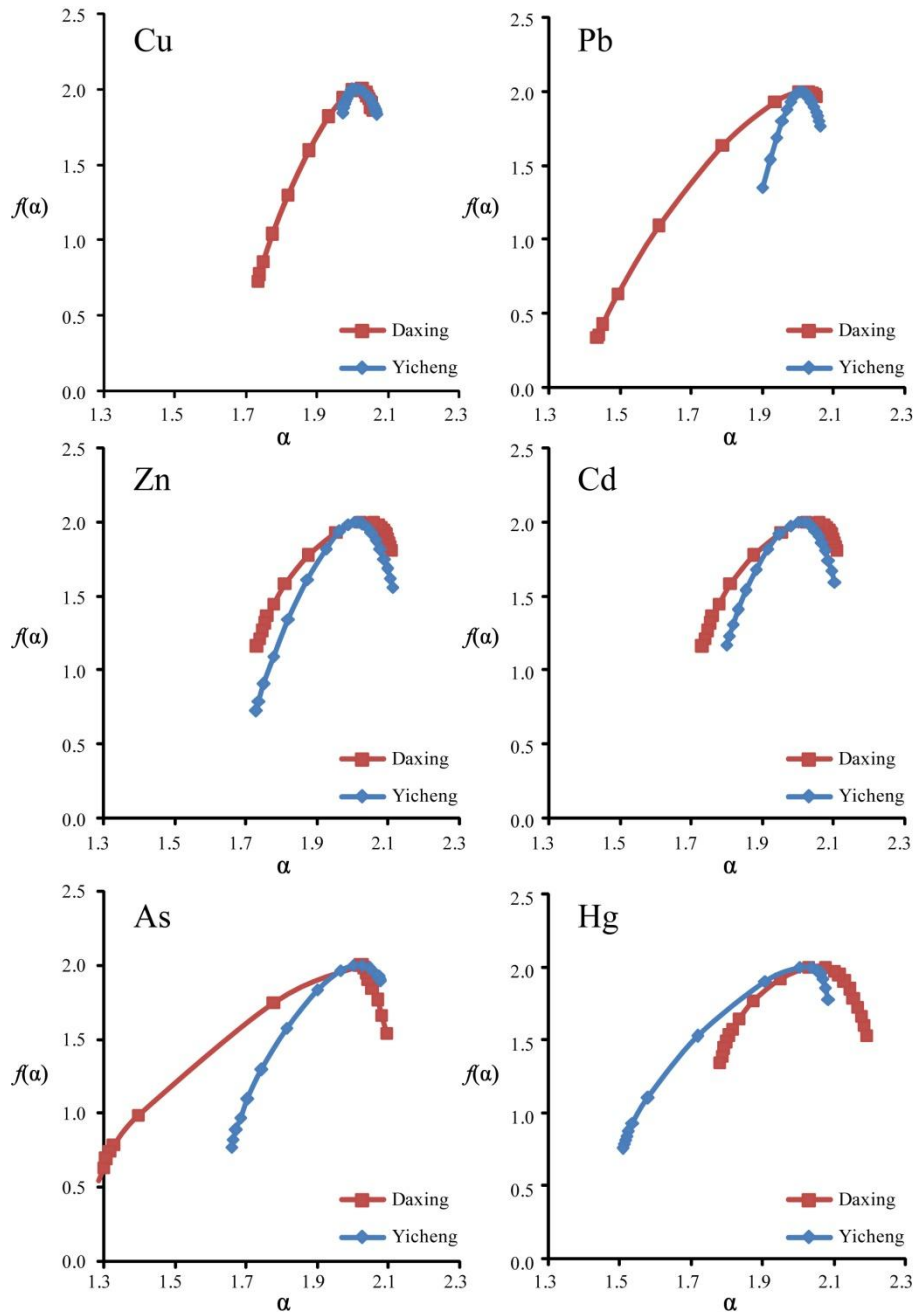
191 **Fig. 2.** Histograms showing the distribution of Cu (a), Pb (b), Zn (c), Cd (d), As (e) and Hg (f)
 192 concentrations within soils from the towns of Daxing and Yicheng.

193

194 **5. Calculation processes of multifractal spectrum and discussion**

195 The multifractal spectra (in the form of an α - $f(\alpha)$ diagram) for the geochemical
196 data are shown in Fig. 3 using a range of q values from -10 to 10 with an interval of
197 1.

198



199

200 **Fig. 3.** Multifractal spectra ($f(\alpha)$ vs α) of the soil geochemical data from the Daxing and Yichen
201 area.

202

203 These multifractal spectra have inverse bell shapes (Fig. 3) and are asymmetric

204 (i.e. $\Delta\alpha_L$ values significantly differ from $\Delta\alpha_R$, equations 5-6) with the exception of the
205 Cu data for soils from the Yicheng area, indicating that the samples containing low
206 and high concentrations of these elements are not evenly distributed within the study
207 area (as is expected for areas containing point source pollutants like factories or
208 animal breeding facilities).

209 The multifractal results given in Table 2 indicate that all of the elements (barring
210 Cu and Pb in the Yicheng area) are characterized by a wide range of α values with
211 $\tau''(1)$ values less than -0.01 and $\Delta f(\alpha)$ values larger than 0.5 , all of which indicate that
212 these elements have highly multifractality within the soils in these two areas. All of
213 the elements analyzed during this study (barring Hg) have higher $\Delta f(\alpha)$ and α values
214 (except Zn) and lower $\tau''(1)$ values in soils from the Daxing area, with Hg having
215 higher $\Delta f(\alpha)$ and α and lower $\tau''(1)$ values in soils from the Yicheng area (Table 2).
216 This suggests that the industrial activities in the Daxing area generate multi-element
217 heavy metal soil contamination, whereas the most significant heavy metal pollution
218 associated with the agricultural activity in the Yicheng area is Hg contamination. The
219 $\Delta f(\alpha)$ and α values of Hg in the Yicheng area are larger than the values for all other
220 elements in this area as well as some of the elements in the Daxing area, indicating
221 both the prevalence and significant degree of agricultural Hg contamination in the
222 Yicheng area, even considering the lower overall (but not maximum) concentrations
223 of Hg within the Yicheng area compared to the Daxing area. This contamination
224 should be considered a priority in terms of remediation, because the interaction
225 between the agricultural activity in the Yicheng area and this Hg pollution
226 could seriously impact human health, as Hg is preferentially concentrated upward in
227 the food chain (e.g. (Jiang et al., 2006)). This means that although contamination in
228 both areas needs to be evaluated further and should be remediated to avoid any
229 deleterious effects such as the heavy metal pollution of people, crops and animals, the
230 fact that the Hg contamination in the Yicheng area may be more bioavailable and may
231 have a larger effect on the population of this region (as a result of the agricultural
232 activity in this area) means it should be considered a priority.

233

234 **Table 2.** Multifractal parameters of the elements analyzed during this study.

Town	Element	α_{\min}	α_{\max}	$\Delta\alpha_L$	$\Delta\alpha_R$	$\Delta\alpha$	$\Delta f(\alpha)$	$\tau''(1)$
Daxing	Cu	1.733	2.057	0.280	0.044	0.324	1.270	-0.015
	Pb	1.439	2.050	0.567	0.044	0.611	1.659	-0.068
	Zn	1.733	2.109	0.288	0.088	0.376	0.841	-0.066
	Cd	1.482	2.285	0.499	0.304	0.803	1.358	-0.066
	As	1.285	2.094	0.739	0.070	0.809	1.490	-0.243
	Hg	1.780	2.191	0.248	0.163	0.411	0.656	-0.079
Yicheng	Cu	1.971	2.067	0.036	0.060	0.096	0.168	-0.007
	Pb	1.900	2.062	0.104	0.058	0.162	0.646	-0.005
	Zn	1.729	2.112	0.275	0.108	0.383	1.275	-0.016
	Cd	1.800	2.103	0.201	0.102	0.303	0.829	-0.023
	As	1.659	2.076	0.343	0.075	0.418	1.224	-0.036
	Hg	1.507	2.084	0.497	0.080	0.577	1.243	-0.096

235

236 In order to compare variations in multifractality, different elements within
 237 Daxing and Yicheng area were sorted by $\Delta\alpha$, $\Delta f(\alpha)$ and $\tau''(1)$ parameters, respectively,
 238 in addition to sorting by basic statistics such as standard deviation and coefficient of
 239 variation values (Table 3). The data shown in Table 3 indicates that the Zn data within
 240 the Daxing area has largest standard deviation value but only a moderate coefficient
 241 of variation, but the $\Delta\alpha$ and $\Delta f(\alpha)$ values for these Zn data are indicative of only weak
 242 multifractality compared to the other heavy metals in the soils within the Daxing area.
 243 In comparison, the Hg data for soils in the Yicheng area yielded the lowest standard
 244 deviation value but the largest $\Delta\alpha$ and $\tau''(1)$ values, indicating these Hg data have
 245 strong multifractality. These differences indicate that the multifractal parameters $\Delta\alpha$,
 246 $\Delta f(\alpha)$ and $\tau''(1)$ reveal new information about the nonlinear variability and the
 247 characteristics of these geochemical data compared to the basic statistics for these
 248 samples. In addition, the data given in Table 3 indicates that these elements have
 249 different orders depending on whether they are sorted by $\Delta\alpha$, $\Delta f(\alpha)$ or by $\tau''(1)$ values,
 250 all of which reflects differing aspects of the multifractality of these data. Here we
 251 consider that $\Delta\alpha$, $\Delta f(\alpha)$ or by $\tau''(1)$ have equal weightings that reflect the overall
 252 multifractality of the data from the study area. As such, the ordering of these elements
 253 by $\Delta\alpha$, $\Delta f(\alpha)$ or by $\tau''(1)$ involved the summation of these values with the summed
 254 ordering then sorted again to compare the overall multifractality of these data.

255

256

Table 3. Elements sorted by multifractal parameters and basic statistic indices.

Town	Element	Order				
		Basic statistics	Multifractal parameters			
		Coefficient of variation	$\Delta\alpha$	$\Delta f(\alpha)$	$\tau''(1)$	Overall*
Daxing	Cu	6	6	4	6	6
	Pb	5	3	1	1	1
	Zn	4	5	5	2	4
	Cd	2	2	3	3	2
	As	1	1	2	5	3
	Hg	3	4	6	4	5
Yicheng	Cu	5	6	6	5	6
	Pb	6	5	5	6	5
	Zn	4	3	1	4	3
	Cd	3	4	4	3	4
	As	2	2	3	2	2
	Hg	1	1	2	1	1

257

Overall: the overall order of $\Delta\alpha$, $\Delta f(\alpha)$ and $\tau''(1)$.

258

259

260

261

262

263

264

265

The overall amount of multifractality within the soil geochemical data for the Daxing area decreases as follows: Pb>Cd>As>Zn>Hg>Cu, whereas the overall amount of multifractality within the soil geochemical data for the Yicheng area decreases as follows: Hg>As>Zn>Cd>Pb>Cu. The overall orders indicates that the Pb and Hg soil data have the highest degree of multifractality in the Daxing and Yicheng areas, respectively, whereas Cu has the weakest multifractality irrespective of the area.

266

267

268

269

270

271

272

273

274

We further analyzed the spatial distribution of contamination within soils from the Daxing and Yicheng areas and evaluated whether there is any significant correlation between multifractality and anthropogenic activity. Filled contour maps showing the distribution of Pb in the Daxing area and Hg and Cu in the Yicheng area were calculated using inverse distance weighted interpolation (Fig. 4–6). These figures show that areas with elevated levels of Pb contamination within the Daxing area are correlated with the location of industrial factories, although interestingly the areas in the upper and lower left hand side of Fig. 4 contain factories but not elevated concentrations of Pb. This indicates that the Pb concentrations in these soils may be

275 dependent on both the presence and type of industry in this area, with some industries
276 more polluting than others, either as a direct result of the differing industries present
277 in this area or as a result of differing (or a lack of in some areas) approaches to
278 lessening environmental impacts. In comparison, the Hg contamination in the Yicheng
279 area is definitely spatially correlated with the location of agricultural breeding
280 facilities. Although the mean concentrations of Hg in soils are greater in the Daxing
281 area, all of the multifractal parameters determined during this study ($\Delta\alpha$, $\Delta f(\alpha)$ and
282 $\tau''(1)$) indicate that the Hg data in the Daxing area has a lower multifractality than
283 the Hg data in the Yicheng area. The Yicheng area is heavily agricultural, meaning
284 that the agricultural activities in this area may be both concentrating Hg as well as
285 contaminating soils. In addition, although the mean concentrations of Hg in the
286 Yicheng area are lower than in the soils in the Daxing area, the former has a higher
287 maximum concentration than the latter, and both areas have significant Hg
288 contamination. Indeed, the contamination in the Yicheng area may be of more concern
289 than the contamination in the Daxing area, as the agricultural activity in the Yicheng
290 area may lead to greater human intake of Hg than from the soils in the mainly
291 industrial Daxing area, a factor that could lead to serious health issues (e.g. Minamata
292 disease) caused by the potential concentration of Hg up the food chain. This indicates
293 that soils in both areas may well require control and remediation.

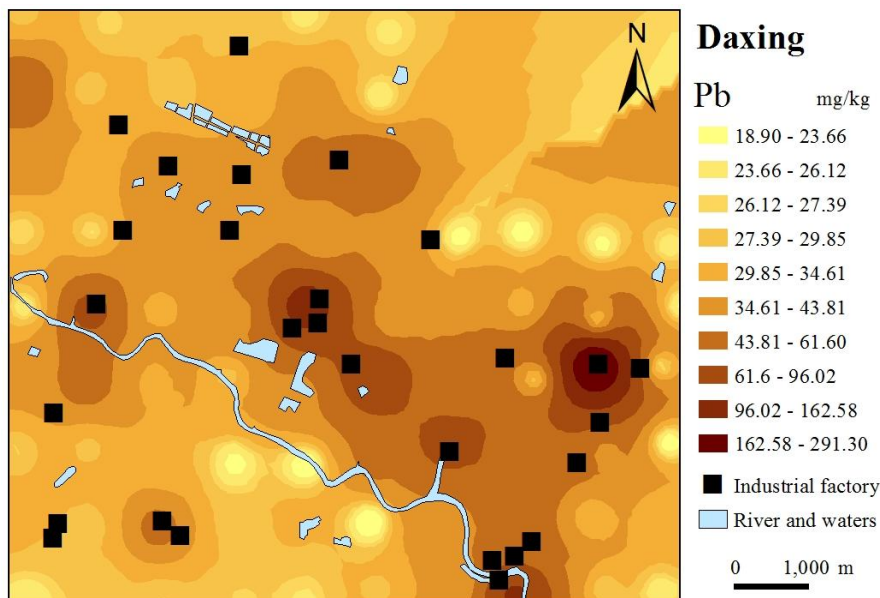
294 This distribution of soils with elevated concentrations of Hg also contrasts with
295 the symmetrical distribution and weakest multifractality for Cu within the Yicheng
296 area (Fig. 3, 5-6). Here, we generated a correlation matrix that compares the
297 relationship between the spatial density of breeding locations in the Yicheng area (Fig.
298 7) and filled contours maps showing the distribution of Hg (Fig. 5) and Cu (Fig. 6) in
299 this region to identify whether there are any spatial correlations between the location
300 of agricultural facilities and areas containing soils with elevated heavy metal
301 concentrations (Table 4). The correlation matrix shows a significant correlation
302 between agricultural facilities and high concentrations of Hg (correlation value =
303 0.434), whereas the location of these agricultural breeding facilities and areas of high
304 Cu concentrations either have no relationship or are negatively correlated (correlation

305 value = -0.064). This indicates that very little Cu has been anthropogenically added
306 (or removed) from the soils in the Yicheng area, suggesting that these soils may
307 contain only natural background concentrations of Cu and that the breeding facilities
308 in this area does not produce significant Cu contamination. The correlation matrix,
309 symmetrical distribution and weakest multifractality for Cu give one clue to the
310 derivation of the Cu contamination in this area is the spatial relationship between Cu
311 contamination and the river in the right hand side of Fig. 6. This may suggest a
312 non-anthropogenic source (e.g. flooding causing the deposition of Cu or some other
313 relationship between water and Cu contamination) for some of the slightly elevated
314 Cu concentrations in this region. In addition, the fact that some breeding facilities are
315 not associated with significant Hg contamination (Fig. 5) suggests again that although
316 there is a relationship between the presence of these facilities and contamination, it
317 may be that the Hg contamination in this area reflects differing types of breeding
318 facilities or differing (or a lack of) approaches to lessening environmental impacts.

319 These results indicate that multifractal modeling and the associated generation of
320 multifractal parameters are a useful approach in the evaluation of heavy metal
321 pollution in soils and the identification of major element of heavy metal
322 contamination. In addition, the differing orders of the multifractality of the
323 geochemical data for soils within the Daxing area and Yicheng area are indicative of a
324 significant difference in the geochemical characteristics (and heavy metal pollution)
325 in the soils within these two areas. This indicates that differing treatment strategy and
326 clean-up approaches to remediating these two polluted areas are needed, rather than a
327 single cover-all strategy and approach to the remediation of heavy metal pollution. A
328 significant number of different remediation approaches can be used to resolve the
329 issues of heavy metal soil contamination (e.g., Bech et al., 2014; Koptsik, 2014).
330 Although somewhat beyond the scope of this study, the multi-element nature of the
331 contamination in the Daxing area means that physical and chemical approaches to
332 remediation (i.e., soil removal, soil vitrification, soil consolidation, electroremediation,
333 or soil washing) are probably well suited for the remediation of heavy metal
334 contaminated soil in this region (especially Pb). In comparison, the differing (i.e.

335 Hg-dominated) type of soil contamination in the Yicheng area could be more
336 efficiently treated using microremediation and phytoremediation, primarily as the
337 agriculture in this area requires a rapid reduction in the mobility and biological
338 availability of heavy metals in the soils (Mulligan et al., 2001; Wang et al., 2006). In
339 addition, the source of the Hg contamination (e.g. fertilizer, fodder, pesticides, water,
340 or some other source remains unclear. Identifying this source is also beyond the scope
341 of this paper although it is also clearly an area for future research, as the identification
342 of the source or sources of this contamination may prevent the future heavy metal
343 pollution of soils in this region.

344



345

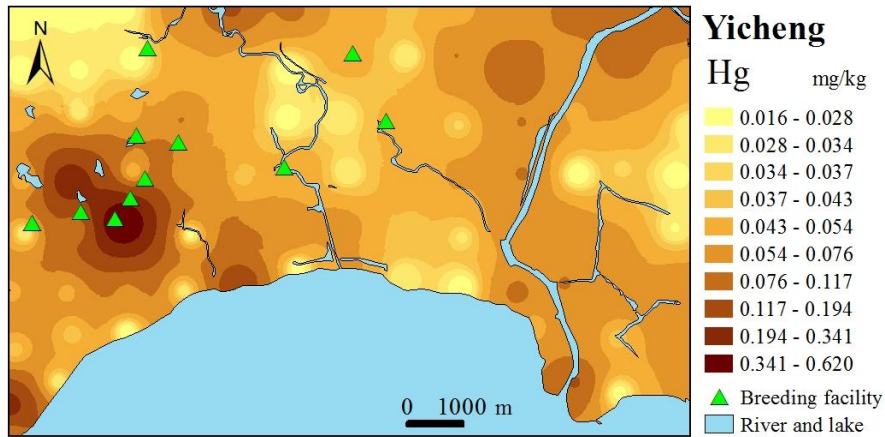
346

Fig. 4. Filled contour map generated by inverse distance weighted interpolation showing the spatial distribution of soil Pb concentrations in the Daxing area.

347

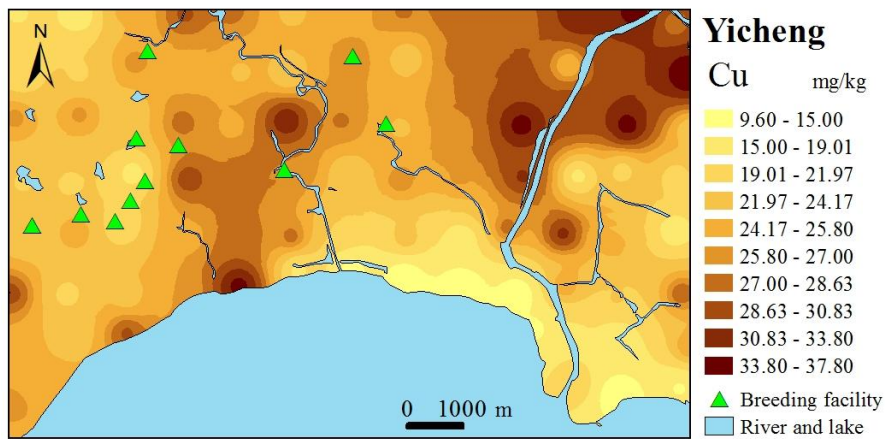
348

349



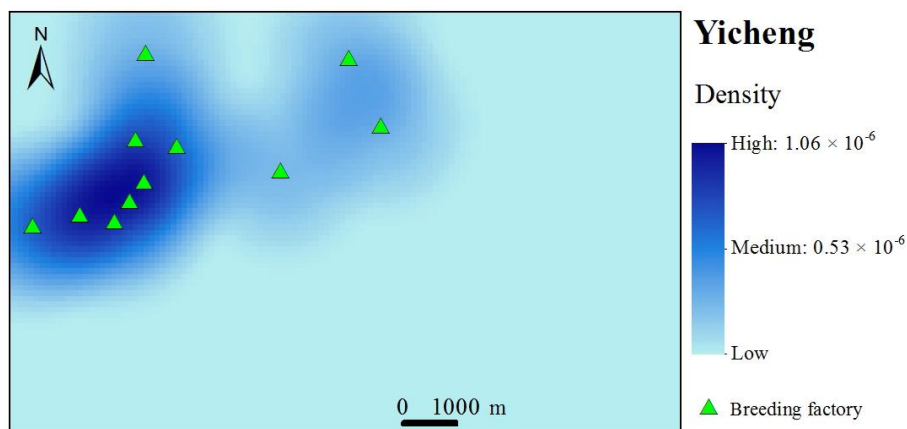
350
351
352
353

Fig. 5. Filled contour map generated by inverse distance weighted interpolation showing the spatial distribution of soil Hg concentrations in the Yicheng area.



354
355
356
357
358

Fig. 6. Filled contour map generated by inverse distance weighted interpolation showing the spatial distribution of soil Cu concentrations and the location of breeding facilities in the Yicheng area



359
360
361
362
363

Fig. 7. Density map of breeding facilities in Yicheng area (generated using the kernel density tool within the ArcGIS software package).

Table 4. Correlation matrix comparing the breeding facility density map and the filled

364

contour maps for Hg and Cu data for the Yicheng area.

Layers	Layer 1	Layer 2	Layer 3
Layer 1	1.00000	0.434	-0.064
Layer 2	0.434	1.000	-0.464
Layer 3	-0.064	-0.464	1.000

365

Layer 1: Density map of breeding factories of Yicheng area (Fig. 8);

366

Layer 2: Filled contour map of Hg concentrations of Yicheng area (Fig. 8);

367

Layer 3: Filled contour map of Cu concentrations of Yicheng area (Fig. 8).

368

The correlations range from +1 to -1, where a positive correlation indicates a direct

369

relationship between the two layers and a negative correlation means that one variable is

370

negatively correlated with the other. A correlation of zero means that two layers are

371

independent of one another.

372

373

5. Conclusions

374

This study focuses on the geochemistry of heavy metal contaminated soils from

375

the Daxing and Yicheng areas, both of which are located close to the city of Hefei, in

376

Anhui Province, China. Multifractal modelling and the resulting multifractal

377

parameters indicate that the soils from the Daxing area have stronger multifractality

378

for Cu, Pb, Zn, Cd and As than soils from the Yicheng area, although the latter have

379

relatively strong multifractality for Hg. The ordering of values for the multifractal

380

parameters $\Delta\alpha$, $\Delta f(\alpha)$ and $\tau''(1)$ indicate the degree of multifractality for the

381

geochemical data for soils within the Daxing area descends as follows:

382

Pb>Cd>As>Zn>Hg>Cu, whereas the overall order in soils within the Yicheng area

383

descends as follows: Hg>As>Zn>Cd>Pb>Cu. In addition, Cu concentrations in soils

384

in the Yicheng area may still have their original (i.e. natural) distribution and may not

385

have been influenced by human activities. These data indicate that the industrial

386

activity concentrated in the Daxing area generates multi-element heavy metal soil

387

contamination whereas the agricultural activity concentrated in the Yicheng area

388

generates Hg-dominated heavy metal soil contamination. The latter is important, as

389

Hg contamination can cause serious health issues (e.g. Minamata disease) and the

390

soils in this area may well require remediation, especially as Hg can be concentrated

391

up the food chain and the Yicheng area is heavily agricultural, indicating that this

392

activity may both be concentrating Hg as well as contaminating soils in this area.

393 The results presented here indicate that multifractal modeling and the associated
394 three multifractal parameters ($\Delta\alpha$, $\Delta f(\alpha)$ and $\tau''(1)$) can efficiently reflect the
395 multifractality caused by industrial and agricultural activities in the Daxing and
396 Yicheng areas, respectively. This in turn indicates that multifractal modeling can be a
397 useful approach in the evaluation of heavy metal pollution in soils and the
398 identification of problematic heavy metals that need remediation in the research area.

399 **Acknowledgements**

400 This research was financially supported by funds from the China Academy of
401 Science "Light of West China" Program, the Fundamental Research Funds for the
402 Central Universities, and the Programme for New Century Excellent Talents in
403 University (Grant No. NCET-10-0324).

404 **References**

- 405 Albanese, S., De Vivo, B., Lima, A., and Cicchella, D.: Geochemical background and
406 baseline values of toxic elements in stream sediments of Campania region (Italy),
407 Journal of Geochemical Exploration, 93, 21-34, 2007.
- 408 Armstrong, H. E. L., Corns, W. T., Stockwell, P. B., O'Connor, G., Ebdon, L., and
409 Evans, E. H.: Comparison of afs and icp-ms detection coupled with gas
410 chromatography for the determination of methylmercury in marine
411 samples. Analytica Chimica Acta, 390, 245-253, 1999.
- 412 Bech, J., Korobova, E., Abreu, M., Bini, C., Chon, H. T., and Pérez-Sirvent, C.: Soil
413 pollution and reclamation, Journal of Geochemical Exploration, 147, 77-79, 2014.
- 414 Buczkowski, S., Hildgen, P., and Cartilier, L.: Measurements of fractal dimension by
415 box-counting: a critical analysis of data scatter, Physica A Statistical Mechanics &
416 Its Applications, 252, 23-34, 1998.
- 417 Caniego, F. J., Espejo, R., Martín, M. A., and José, F. S.: Multifractal scaling of soil
418 spatial variability, Ecological Modelling, 182, 291-303, 2005.
- 419 Cheng, Q.: The perimeter-area fractal model and its application to geology,
420 Mathematical Geology, 27, 69-82, 1995.
- 421 Cheng, Q.: The gliding box method for multifractal modeling, Computer &

422 Geosciences, 25, 1073-1079, 1999.

423 Cheng, Q.: Selection of Multifractal Scaling Breaks and Separation of Geochemical
424 and Geophysical Anomaly, Journal of China University of Geosciences, 1, 54-59,
425 2001.

426 Cheng, Q.: Multifractal modelling and spectrum analysis: Methods and applications to
427 gamma ray spectrometer data from southwestern Nova Scotia, Canada, Science in
428 China Series D: Earth Sciences, 49, 283-294, 2006.

429 Dathe, A., Tarquis, A. M., and Perrier, E.: Multifractal analysis of the pore- and
430 solid-phases in binary two-dimensional images of natural porous structures,
431 Geoderma, 134, 318–326, 2006.

432 Deng, J., Wang, Q., Wan, L., Liu, H., Yang, L., and Zhang, J.: A multifractal analysis
433 of mineralization characteristics of the Dayingezhuang disseminated-veinlet gold
434 deposit in the Jiaodong gold province of China, Ore Geology Reviews, 40, 54–64,
435 2011.

436 Gómez-Ariza, J. L, Sánchez-Rodas, D., Giráldez, I., and Morales, E.: A comparison
437 between ICP-MS and AFS detection for arsenic speciation in environmental
438 samples, Talanta, 51, 257-268, 2000.

439 Gonçalves, M. A.: Characterization of Geochemical Distributions Using Multifractal
440 Models, Mathematical Geology, 33, 41-61, 2000.

441 Guillén, M. T., Delgado, J., Albanese, S., Nieto, J. M., Lima, A., and De Vivo, B.:
442 Environmental geochemical mapping of Huelva municipality soils (SW Spain) as
443 a tool to determine background and baseline values, Journal of Geochemical
444 Exploration, 109, 59-69, 2011.

445 Halsey, T.C., Jensen, M.H., Kadano, L.P., Procaccia, I., and Shraiman, B.I.: Fractal
446 measures and their singularities: the characterization of strange sets. Physical
447 Review, A, 33 (2), 1141-1151, 1986.

448 Jennane, R., Ohley, W. J., Majumdar, S., and Lemineur, G.: Fractal analysis of bone
449 X-ray tomographic microscopy projections, IEEE Transactions on Medical
450 Imaging, 20, 443-449, 2001.

451 Jiang, G. B., Shi, J. B., and Feng, X. B.: Mercury Pollution in China, Environmental

452 Science & Technology, 40, 3672-3678, 2006.

453 Koptsik, G. N.: Modern approaches to remediation of heavy metal polluted soils: A
454 review, *Eurasian Soil Science*, 47, 707-722, 2014.

455 Kravchenko, A., Boast, C., and Bullock, D.: Multifractal analysis of soil spatial
456 variability, *Agronomy Journal*, 91, 1033-1041, 1999.

457 Leyval, C., Turnau, K., and Haselwandter, K.: Effect of heavy metal pollution on
458 mycorrhizal colonization and function: physiological, ecological and applied
459 aspects, *Mycorrhiza*, 7, 139-153, 1997.

460 Lima, A., De Vivo, B., Cicchella, D., Cortini, M., and Albanese, S.: Multifractal IDW
461 interpolation and fractal filtering method in environmental studies: an application
462 on regional stream sediments of (Italy), Campania region, *Applied Geochemistry*,
463 18, 1853-1865, 2003.

464 Lopes, R., and Betrouni, N.: Fractal and multifractal analysis: A review, *Medical
465 Image Analysis*, 13, 634-649, 2009.

466 Luo, C., Liu, C., Yan, W., Xiang, L., Li, F., Gan, Z., and Li, X.: Heavy metal
467 contamination in soils and vegetables near an e-waste processing site, South
468 China, *Journal of Hazardous Materials*, 186, 481-490, 2011.

469 Mulligan, C., Yong, R., and Gibbs, B. F.: Remediation technologies for
470 metal-contaminated soils and groundwater: an evaluation. *Engineering Geology*,
471 60, 193-207, 2001,

472 McGrath, D., Zhang, C., and Carton, O. T.: Geostatistical analyses and hazard
473 assessment on soil lead in Silvermines area, Ireland, *Environmental Pollution*,
474 127, 239-248, 2004.

475 Nazarpour, A., Omran, N. R., Paydar, G. R., Sadeghi, B., Matroud, F., and Nejad, A.
476 M.: Application of classical statistics, logratio transformation and multifractal
477 approaches to delineate geochemical anomalies in the Zarshuran gold district,
478 NW Iran, *Chemie der Erde - Geochemistry*, 75, 117-132, 2014.

479 Pascual, M., Ascioti, F., and Caswell, H.: Intermittency in the plankton: a multifractal
480 analysis of zooplankton biomass variability, *Journal of Plankton Research*, 17,
481 167-168, 1995.

482 Salvadori, G., Ratti, S. P., and Belli, G.: Fractal and multifractal approach to
483 environmental pollution, *Environmental Science & Pollution Research*, 4, 91-98,
484 1997.

485 Schertzer, D., Lovejoy, S., Schmitt, F., Chigirinskaya, Y., and Marsan, D.: Multifractal
486 Cascade Dynamics and Turbulent Intermittency, *Fractals-complex Geometry*
487 *Patterns & Scaling in Nature & Society*, 5, 427-471, 2011.

488 Scheuring, I., and Riedi, R.: Application of multifractals to the analysis of vegetation
489 pattern, *Journal of Vegetation Science*, 5, 489-489, 1994.

490 Tarquis, A. M., Mcinnes, K. J., Key, J. R., Saa, A., Garc á, M. R., and D áz, M. C.:
491 Multiscaling analysis in a structured clay soil using 2D images, *Journal of*
492 *Hydrology*, 322, 236-246, 2006.

493 Thomas, K., and Stefan, S.: Estimate of heavy metal contamination in soils after a
494 mining accident using reflectance spectroscopy, *Environmental Science &*
495 *Technology*, 36, 2742-2747, 2002.

496 Wang, Y., and Greger, M.: Use of iodide to enhance the phytoextraction of
497 mercury-contaminated soil. *Science of the Total Environment*, 368, 30-39, 2006.

498 Wang, Y. P., Shi, J. Y., Wang, H., Lin, Q., Chen, X. C., and Chen, Y. X.: The influence
499 of soil heavy metals pollution on soil microbial biomass, enzyme activity, and
500 community composition near a copper smelter. *Ecotox Environ Safe*,
501 *Ecotoxicology & Environmental Safety*, 67, 75-81, 2007.

502 Wendt, H., Roux, S. G., Jaffard, S., and Abry, P.: Wavelet leaders and bootstrap for
503 multifractal analysis of images, *Signal Processing*, 89, 1100–1114, 2009.

504 Xie, S., Cheng, Q., Xing, X., Bao, Z., and Chen, Z.: Geochemical multifractal
505 distribution patterns in sediments from ordered streams, *Geoderma*, 160, 36-46,
506 2010.

507 Yuan, F., Li, X., Jowitt, S. M., Zhang, M., Jia, C., Bai, X., and Zhou, T.: Anomaly
508 identification in soil geochemistry using multifractal interpolation: A case study
509 using the distribution of Cu and Au in soils from the Tongling mining district,
510 Yangtze metallogenic belt, Anhui province, China, *Journal of Geochemical*
511 *Exploration*, 116-117, 28-39, 2012.

512 Yuan, F., Li, X., Zhou, T., Deng, Y., Zhang, D., Xu, C., Zhang, R., Jia, C., and Jowitt,
513 S. M.: Multifractal modelling-based mapping and identification of geochemical
514 anomalies associated with Cu and Au mineralisation in the NW Junggar area of
515 northern Xinjiang Province, China, *Journal of Geochemical Exploration*, 154,
516 252-264, 2015.

517 Zuo, R., Carranza, E. J. M., and Cheng, Q.: Fractal/multifractal modelling of
518 geochemical exploration data, *Journal of Geochemical Exploration*, 122, 1-3,
519 2012.

520 Zuo, R.: Identification of geochemical anomalies associated with mineralization in the
521 Fanshan district, Fujian, China, *Journal of Geochemical Exploration*, 139,
522 170–176, 2014.